Neutron emission in deep-inelastic collisions induced by ^{86}Kr on ^{166}Er at 5.7, 7.0, and 7.9 MeV/nucleon

Y. Eyal, A. Gavron, I. Tserruya, Z. Fraenkel, Y. Eisen, and S. Wald
Weizmann Institute of Science, Rehovot, Israel

R. Bass, C. R. Gould,* G. Kreyling, R. Renfordt, K. Stelzer, and R. Zitzmann
Institut für Kernphysik, University of Frankfurt, Frankfurt, West Germany

A. Gobbi, U. Lynen,† H. Stelzer, I. Rode, and R. Bock
GSI, Darmstadt, West Germany

(Received 6 July 1979)

Neutron emission associated with deep-inelastic collisions of 496-, 602-, and 675-MeV ^{86}Kr with ^{166}Er has been studied as a function of kinetic energy loss, fragment mass, and neutron scattering angles. The major de-excitation process is neutron evaporation from fully accelerated fragments. The excitation energy is shared between the fragments in proportion to their mass, indicating energy equilibration in the intermediate dinuclear composite system for the completely damped as for the quasielastic components. Within limits imposed by the systematic uncertainties, the angular and velocity distributions of the neutrons in the laboratory frame are consistent with isotropic emission of neutrons in the c.m. frame of the fragments. We find no evidence for pre-equilibrium effects. The observed multiplicities and energy spectra of the neutrons are consistent with predictions of statistical-model calculations.

[NUCLEAR REACTIONS ^{166}Er(^{86}Kr, A_L)A_H E_{lab}=496, 602, and675 MeV; $66 \leq A_L \leq 126$, $A_H = 252 - A_L$, $\theta \sim 21°-75°$, $-250 \leq Q$ value ≤ 0 MeV; measured $\sigma_n(E_{lab}, Q$ value, θ, A_L,A_H,E_n, θ_n, ϕ_n); deduced neutron c.m. energy spectra, out-of-plane anisotropy and multiplicities; degree of energy equilibration.]

I. INTRODUCTION

The investigation of prompt neutron and charged-particle emission associated with deep-inelastic collisions between very heavy ions is of importance to the understanding of the de-excitation processes involved in the collision. Of particular interest is the distinction between particle emission which occurs at the instant of the collision, when transfer of mass, momentum, and energy takes place, and particle evaporation from the excited reaction products. The particles of the first group, if found, may shed light on the nature of the short-lived highly excited transient configurations produced in the region of strongly overlapping nuclear matter. The investigation of the particles of the second group, particularly their type, number, angular distributions, and kinetic energy spectra, may allow the determination of the total excitation energy deposited, the sharing of excitation energy between the fragments, and may supply information on the time scale of energy equilibration. For highly excited heavy ions, neutron emission is expected to dominate in the de-excitation process, as determined by studies of (HI, xn) reactions and fission.

Recently a number of investigations have been published in which the neutron multiplicity as a function of fragment mass and kinetic energy was measured.[1-5] The purpose of these experiments was to detect possible neutron emission from the composite nuclear system prior to the separation of the two heavy fragments and to determine the excitation energy of the two fragments after separation by measuring the number of neutrons emitted from them. Preliminary experiments of Peter *et al.*[1] and Gould *et al.*[2] seemed to indicate that a fraction of the neutrons are emitted prior to the separation of the fragments. However, the results of our more detailed experiment[3] as well as those of Hilscher *et al.*[4] and Tamain *et al.*[5] are consistent with the assumption that all the neutrons are emitted from the fragments after their separation and that the excitation energy is shared between the fragments in proportion to their masses. The number of neutrons emitted from each fragment can also be determined indirectly, for example by measuring simultaneously the angle, charge, mass, and kinetic energy of one of the fragments as was done by Plasil *et al.*[6] and Babinet *et al.*[7] or by measuring the energy and angle of both fragments and the charge of one of them

(Cauvin *et al.*, Ref. 8). Finally Schmitt *et al.*[9] presented evidence for energy thermalization in deep-inelastic processes from the simultaneous measurement of both deep-inelastic fragments emitted in these reactions.

In this work we report on a study of neutron emission associated with deep-inelastic collisions of ^{86}Kr on ^{166}Er at 5.7, 7.0, and 7.9 MeV/nucleon. First results obtained at 7.0 MeV/nucleon were presented in Ref. 3. At each bombarding energy, the neutron yield was measured as a function of total kinetic energy (TKE) loss, fragment mass, and fragment and neutron emission angles. The experimental arrangement which was used to detect neutrons in coincidence with the two complementary heavy reaction fragments, is described in Sec. II. The method of data analysis is presented in Sec. III, and the evaporation calculations are described in Sec. IV. The experimental data, discussed in Sec. V, include the following results: (i) velocity spectra of neutrons in the laboratory frame, (ii) average neutron multiplicities as functions of bombarding energy, TKE loss, and fragment mass, and (iii) neutron kinetic energy spectra in the c.m. frame of the fragments. The discussion (Sec. VI) involves a detailed comparison of the results of the evaporation calculations with experiment. Briefly, we conclude that the total observed TKE loss is transformed into excitation energy of the fragments. The excitation energy is shared between the fragments in proportion to their mass, indicating that equilibration of the excitation energy in the intermediate composite system is achieved during the collision time. The angular distributions and the velocity spectra of the neutrons in the laboratory frame are consistent with isotropic emission of neutrons in the c.m. frame of the fully accelerated fragments. Within limits imposed by systematic uncertainties we find no evidence for pre-equilibrium neutron emission. Section VII gives a short summary of the present work.

II. EXPERIMENTAL ARRANGEMENT

The experiments were performed with 496-, 602-, and 675-MeV beams of ^{86}Kr provided by the UNILAC accelerator at GSI, Darmstadt. We made use of the bunched-beam facility of the UNILAC which yielded 250-ps-wide beam pulses at 37-ns intervals. These pulses provided the reference timing signals for all time-of-flight (TOF) measurements. In order to minimize the neutron and γ-ray background in the vicinity of the detection system, excessive collimation of the beam by mechanical means was avoided. The target consisted therefore of a 3-mm-wide vertical ^{166}Er strip, evaporated on a carbon foil 15 mm in diameter. The target thickness was 250 μg/cm^2 and its isotopic composition 96.2% ^{166}Er, 2.8% ^{167}Er, and 1.0% of other stable Er isotopes. The thickness of the carbon foil was 25 μg/cm^2. The target was placed in the center of a 60-cm-diam. scattering chamber. This chamber consisted of a 2-cm-thick aluminum base, located 15 cm below the beam axis, and of a 3-mm-thick dome-shaped aluminum cover especially designed to minimize neutron scattering. The beam stop, located ~4 m downstream of the target, consisted of a thick tantalum plate. The beam stop was surrounded by paraffin, iron, and lead.

The experiment was designed to detect neutrons in coincidence with the two fragments. The experimental arrangement is shown in Fig. 1. The two complementary heavy reaction products were detected in a pair of 8×10 cm^2 two-dimensional position-sensitive parallel-plate avalanche counters (PSPP).[10] These counters were placed on opposite sides of the beam axis in the forward hemisphere of the scattering chamber. The counter-target distances were ~21 cm. The left PSPP counter covered an angular range of ~24° in the

	Θ (deg)	Φ (deg)		Θ (deg)	Φ (deg)
L	55	0	R	43	180
FL	13	0	FR	13	180
BL	82	0	BR	62	180
OL	58	50	OR	55	123

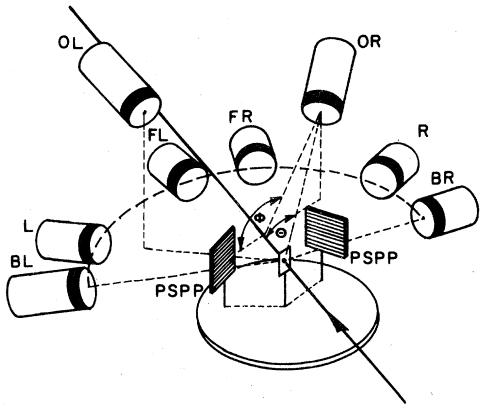

FIG. 1. The experimental arrangement: PSPP are the position-sensitive parallel-plate avalanche counters for the two heavy fragments; FL and FR are the forward neutron counters; BL and BR, the backward neutron counters; OL and OR, the out-of-plane neutron counters; and L and R, the "main" counters positioned approximately behind the PSPP's. The table gives the exact polar (θ) and azimuthal (ϕ) angles of the neutron detectors.

laboratory and subtended a solid angle of ~175 msr at the target. The right (defining) PSPP counter covered an angular range of ~22° in the laboratory and subtended a solid angle of ~60 msr. The effective solid angle of the right PSPP counter was reduced in order to increase the ratio between the fragment-fragment coincidence events and the singles events. The geometries of the PSPP counters at the three bombarding energies are listed in Table I. Geometries C, D, F, and H were adjusted to intercept mainly strongly damped events. Geometries A, B, E and G served to detect mainly quasi-elastic collisions as well as the elastic scattering.

Details about the construction and operation of the PSPP counters were presented in Ref. 10. The walls of the detector housing were made of 1-mm-thick aluminum sheets. This was done in order to minimize scattering and absorption of neutrons. The neutron absorption by the PSPP's was checked experimentally (see Sec. III B). Each PSPP counter provided five signals per event: four position signals (see Ref. 10) and the timing signal for the fragment TOF measurement, relative to the bunched beam.

Neutrons were detected in coincidence with both fragments at eight fixed angles in space. The neutron counters consisted of 5.1-cm-thick NE-213 liquid scintillators of 11.3 or 12.6 cm diameter, covered in front and at the circumference by 3-mm-thick lead shields to reduce γ background. The counters were placed at distances of ~75 cm from the target. Details of the exact locations are presented in Fig. 1. Two detectors labeled L (left) and R (right) were placed in the direction of the detected fragments, the detectors FL and FR were placed at forward angles, the detectors BL and BR at backward angles, and counters OL and OR out-of-plane with respect to the direction of the two fragments. For each scintillator event three signals were recorded: the timing signal for the TOF measurement, a pulse shape analyzer signal, and the pulse-height signal from the photomultiplier. Fragment-fragment coincidence events and fragment-fragment-scintillator coincidence events were recorded event by event with the aid of an on-line multiparameter data acquisition system.[11] Each fragment-fragment event in coincidence with at least one scintillator detector was recorded on magnetic tape and was marked with a pattern word identifying the scintillation counters which fired. Triple- (or more) scintillator events ($\lesssim$0.5% of the total number of scintillator events) were neglected in the analysis. The number of recorded fragment-fragment coincidence signals was reduced electronically with the aid of a scaling-down unit in order to minimize the dead time of the data acquisition system. The magnitude of the scaling down factor varied from 2 to 20, depending mainly on the geometry of the PSPP counters.

III. DATA ANALYSIS

A. Determination of the primary mass and kinetic energy of the fragments

The analysis was based on the assumption of two-body reaction kinematics. This assumption is strongly supported by the results of the present work. However, recoil effects caused by in-flight particle emission (which alter slightly the primary velocities and directions of the fragments) must be considered. These effects cause dispersion of the masses and kinetic energies of the fragments irrespective of the accuracy of the measurement. We have measured the scattering angles and velocities of both fragments while only three of those quantities are sufficient for the determination of

TABLE I. Incident energies of ^{86}Kr beams, grazing angles, and ranges of polar angles θ covered by the two PSPP counters. The left and right PSPP counters subtended solid angles of ~175 msr and ~60 msr, respectively, at the target.

Lab energy (MeV)	c.m. energy (MeV)	Lab grazing angle (deg)	Geometry	Range of θ (deg) Left PSPP	Right PSPP
496	326	53	A	46.5–70.5	37.5–59.5
			B	46.5–70.5	31.5–53.5
			C	39.0–63.0	31.5–53.5
			D	29.0–53.0	31.5–53.5
602	396	37	E	51.0–75.0	25.0–47.0
			F	34.0–58.0	25.0–47.0
675	445	31	G	49.0–73.0	21.5–43.5
			H	32.0–56.0	21.5–43.5

the primary masses and kinetic energies. In order to choose the analysis procedure which minimizes the dispersion due to in-flight particle emission, we have performed Monte Carlo calculations which simulate the detection of binary fragments from strongly damped events, taking into account the angular and velocity dispersions due to isotropic emission of neutrons and charged particles. These calculations show that the best mass and kinetic-energy resolution is achieved by basing the analysis on the measured scattering angles of the two fragments and the velocity of the faster fragment.

The fragment-fragment coincidence data were processed event by event using a procedure similar to that of Ref. 10. The combined angular resolution of the two PSPP counters, as determined by elastic scattering measured at all possible reaction planes, was 0.9° full width at half maximum (FWHM). This value includes the effect of the finite size of the beam spot. The experimental mass and energy resolution, as measured by the elastic peak at 602-MeV beam energy was 6 u FWHM in mass and 35 MeV FWHM in the TKE of the outgoing fragments. The additional uncertainties in the mass and TKE determinations due to in-flight particle emission increase with increasing TKE loss. According to the simulation calculations described above (see also Sec. IV and Ref. 12), this broadening is in the range of ~3–9 u FWHM in mass and ~12–30 MeV FWHM in TKE. The fragment velocities and directions were corrected for the recoil momenta imparted to them by detected neutrons.[13] This correction was found to be negligible for the determination of the neutron multiplicity.

B. Neutron detection

The kinetic energies of the neutrons were determined from their TOF, measured relative to the bunched beam. A typical TOF spectrum is shown in Fig. 2. The combined time resolution for the NE-213 counters and the beam pulses, as determined by the width of the γ peak, was ~1 ns FWHM. The separation between neutrons and γ rays was obtained by the TOF method. Further discrimination against delayed γ rays [such as γ rays produced by $(n,n'\gamma)$ reactions] was achieved with the aid of pulse shape analysis. An example is shown in Fig. 3.

The intrinsic efficiency of the neutron counters as a function of the neutron velocity and pulse-height-discrimination level was determined by the method of Drosg.[14] In our off-line analysis we used a lower discrimination level of 1.6 MeV. We estimate that for the neutron counters positioned

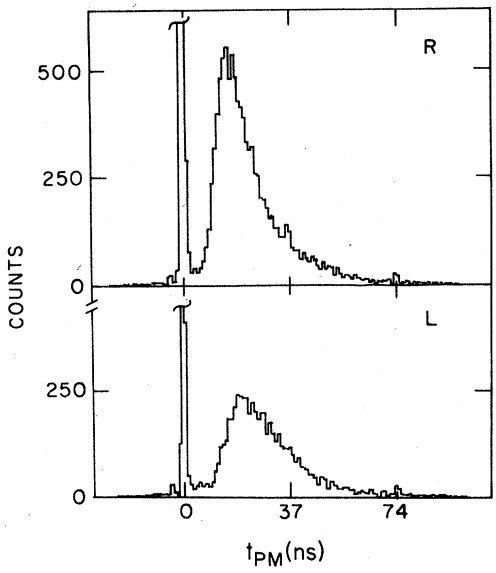

FIG. 2. On-line display of time-of-flight spectra of the "main" neutron detectors R and L. The sharp peak at $t_{pm}=0$ is the prompt gamma peak. The neutron events are well separated from the prompt gamma peak. The small peaks at $t_{pm}=37$ ns and 74 ns are due to prompt gamma ray emitted in subsequent beam pulses and are indicative of the amount of random events. Since the R counter detected mostly the lighter (and faster) fragment, its neutron peak is shifted to smaller t_{pm} (higher neutron velocity).

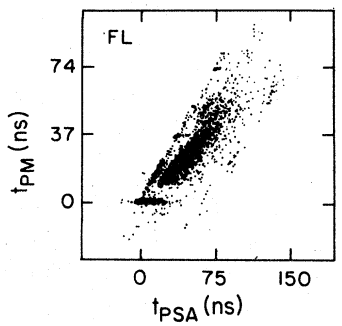

FIG. 3. On-line two-dimensional display of time spectra obtained with neutron counter FL: t_{pm} and t_{psa} are the time differences between the beam pulse signal and the photomultiplier timing and pulse-shape-analyzer signals, respectively. The accumulation of events at $t_{pm}=t_{psa}=0$ are the prompt gamma events and the line $t_{pm}=t_{psa}$ corresponds to subsequent gamma events which could not have separated from the neutron events (the main accumulation of points to the right of the gamma line and well separated from it) without pulse-shape analysis. The small "peaks" in the gamma line at $t_{pm}=t_{psa}=37, 74$ ns are due to gamma events from subsequent beam pulses and are indicative of the amount of random events.

in the direction of the fragments this lower level was sufficient to account for ~100% of the neutrons emitted by the light fragment and for ~95% of the neutrons emitted by the heavy fragment assuming statistical evaporation. The systematic uncertainty associated with our reliance on the general efficiency curve of Drosg is ±5%. The error associated with the uncertainty in the discrimination level (which is the main source of error) is energy dependent. (The error bars in Fig. 1 of Ref. 3 show this effect.) The overall effect on the total multiplicity is estimated to be ±10%.

The neutron absorption by the PSPP counters was measured with 3- and 8-MeV neutrons produced by the ^{7}Li(p,n) reaction. The attenuation in the direction of the neutron counters was found to be 0–8% except in the direction of the counter labeled *BR*. The efficiency of this counter was considerably perturbed in some of the measurements by the flange mounted on the large-angle side of the right PSPP detector housing and by the target frame. This counter was disregarded in the analysis.

Most of the neutron yield in the TOF spectra was observed within the first time interval (0–37 ns) immediately following the correct beam pulse. A fraction of the low-energy neutrons reached the NE-213 counters during the next time interval (37–74 ns). We used neutron events observed at other beam intervals to subtract random events from the relevant velocity intervals. This correction was <1% (see Fig. 2).

C. Neutron multiplicity and angular distribution

The number of neutrons $N(V_{lab})$ as a function of the neutron laboratory velocity V_{lab} per single deep-inelastic event, expressed as $d^2N(V_{lab})/d\Omega dV_{lab}$ (the neutron laboratory velocity spectrum), was obtained for the eight NE-213 counters.

The analysis of the neutron velocity spectra may conveniently be divided into three steps:

(1) First, we analyzed the spectra measured in two "primary" counters assuming that the neutrons detected in these counters were *emitted isotropically in the c.m. system of the two fully accelerated fragments*. Based on this assumption we calculated the number and energy spectra of the neutrons emitted by the two fragments as a function of the fragment masses and total kinetic energy of the fragments. We used the neutron counters R and L (positioned approximately in the direction of the fragment counters) as the "primary" counters. The large focusing effect of the fragment motion on the angular distribution of the neutrons in the laboratory frame facilitates the separation of the contribution of the neutrons emitted by each of the two complementary fragments. The analysis was similar to that described by Fraenkel *et al.*[15] It assumes that the neutrons detected in counters L or R were emitted by the fragment detected in their respective direction, but corrects the results to first order for the contribution from the complementary fragment. These corrections were typically ~5%.

(2) In the next step the neutron spectra measured by the rest of the neutron counters (FL, FR, BL, OL, and OR) were used to verify the assumption that all neutrons are emitted isotropically from the fully accelerated fragments. For this purpose we computed the predicted neutron energy spectra at the five counters by transforming the neutron spectra measured by the "primary" counters L and R to the laboratory angles of the other five counters and comparing these "projected" spectra with the spectra measured by these counters. A deviation from the assumption of isotropic emission, such as "pre-equilibrium" emission from the composite nuclear system, would manifest itself in a discrepancy between the "projected" and measured spectra of the five counters.

In order to check the accuracy of our analysis procedure a Monte Carlo simulation code was written. The code simulates (i) fragment distributions of strongly damped collisions, (ii) neutron emission by fully accelerated fragments, and (iii) neutron detection. By comparing the number of neutrons determined from the analysis with the number given as input we determined that the error in the extracted values of the neutron multiplicity due to systematic errors in the analysis procedure is ~5%.

(3) In the third step of the analysis we compared the experimental c.m. neutron spectra with calculated results based on the assumptions: (i) The total excitation energy of the composite system is divided between the two fragments according to their mass. (ii) The deexcitation of the two fragments proceeds through the evaporation of neutrons and charged particles as predicted by the statistical model.

IV. EVAPORATION CALCULATIONS

The evaporation calculations were performed with the aid of the multistep Monte Carlo code JULIAN[16]. Angular momentum dependent decay widths for n, p, and α particles were computed according to the Hauser-Feshbach formalism. In addition, γ-ray emission and fission were included. Transmission coefficients for neutrons and protons were calculated using optical potentials of Ref. 17, and for α particles those of Ref. 18. For

γ-ray emission transitions up to multipolarity 2 were taken into account. We used averaged empirical transition strengths taken from Ref. 19. Fission was allowed to compete with particle and γ-ray emission at any step along the evaporation cascade. The fission width was calculated by the formalism described in Ref. 20, using rotating-liquid-drop fission barriers.[21] Level densities were calculated with the formalism of Gilbert and Cameron.[22]

The quantities obtained by the code which are relevant for the present study are the following:

(i) Particle multiplicities as functions of fragment atomic number, mass number, excitation energy, and spin.

(ii) Particle kinetic energy spectra in the c.m. frame of the fragment.

(iii) Particle out-of-plane angular distributions in the c.m. frame of the fragment assuming initial alignment of the fragment spin perpendicular to the reaction plane.

(iv) The random deflection of the final fragment residue and the dispersion in its velocity caused by in-flight particle emission which were used in the simulation calculations described in Sec. III A.

V. EXPERIMENTAL RESULTS

Experimental neutron laboratory velocity spectra at forward angles (counters FL and FR), backward angle (counter BL), and out-of-plane angles (counters OL and OR), measured at the 675-MeV bombarding energy, are presented in Fig. 4. The spectra are averaged over fragment masses between 66 and 168 and over the range 170–220 MeV in the c.m. TKE of the outgoing fragments. These spectra are compared with projected spectra obtained with counters R and L, assuming isotropic evaporation of neutrons in the c.m. frame of the fragments.

Typical neutron kinetic energy spectra in the c.m. frame of the projectilelike and targetlike fragments are shown in Fig. 5. The points were obtained with counters L and R.

Measured average neutron multiplicities as functions of the fragment mass and TKE of the outgoing fragments are displayed in Figs. 6–8 for the 496-, 602-, and 675-MeV bombarding energies. The data were obtained with counters L and R. The highest TKE intervals in Figs. 7 and 8 pertain to quasielastic scattering for which the yield of nearly symmetric mass division is very small.

The errors shown in Figs. 4–8 pertain to statistical uncertainties only. The additional systematic error associated with the uncertainty in the efficiencies of the neutron counters is estimated to be ±10%. Typical values for the mass and energy resolutions, including dispersion effects caused by in-flight particle emission (see Sec. III A), are estimated to be ~10 u FWHM in mass and ~50 MeV FWHM in c.m. TKE of the outgoing fragments.

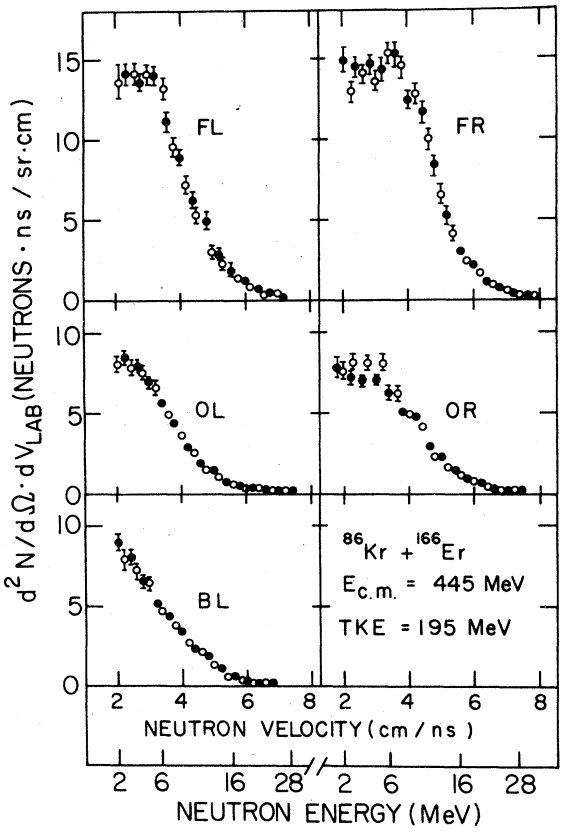

FIG. 4. Measured (full circles) neutron laboratory velocity spectra at forward angles (counters FL and FR), backward angle (counter BL), and out-of-plane (counters OL and OR) compared with projected (open circles) spectra obtained with counters L and R assuming isotropic evaporation of neutrons in the c.m. frame of the fragments. The spectra are averaged over fragment masses between 66 and 168 and over the range 170–220 MeV in c.m. TKE of the outgoing fragments measured at $E_{c.m.}$ = 445 MeV.

VI. DISCUSSION

A. Neutron velocity spectra at the laboratory frame

Inspection of Fig. 4 reveals that essentially all the neutron yield at forward and backward angles, as well as at out of plane, agrees with the assumption of isotropic neutron evaporation from fully accelerated fragments. Within systematic errors (±15%) similar results were obtained for other TKE intervals at the 675-MeV bombardment as well as in the experiments with the 602-MeV

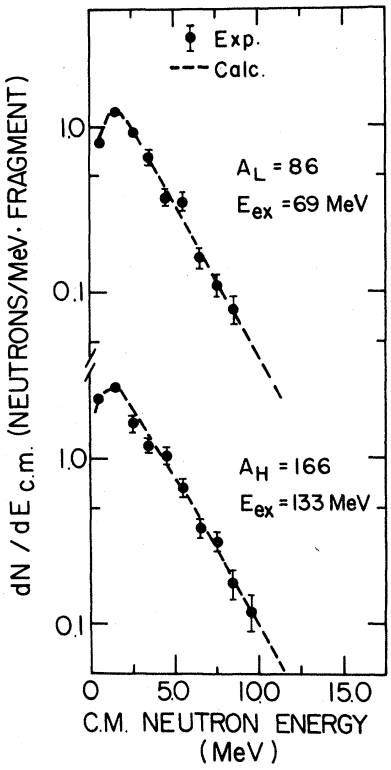

FIG. 5. Neutron kinetic energy spectra in the c.m. frame of the projectilelike (A_L) and targetlike (A_H) fragments (full circles) compared with spectra calculated according to the statistical model (dashed curves). The data points were obtained with counters L and R at $E_{c.m.}$ = 396 MeV, and averaged over the range of 181–223 MeV in total excitation energy and over intervals of 8 u in mass centered around A_L = 86 and A_H = 166. The calculated spectra are for ^{86}Kr and ^{166}Er excited to 69 MeV and 133 MeV, respectively.

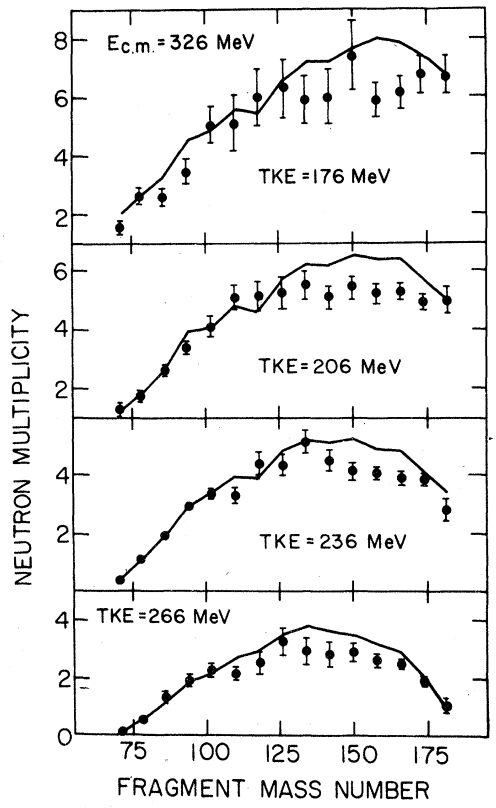

FIG. 6. Neutron multiplicities at four TKE intervals as functions of the fragment primary mass measured for the reaction ^{86}Kr on ^{166}Er at $E_{c.m.}$ = 326 MeV. The points were obtained with counters L and R. The neutron multiplicities are averaged over intervals of 8 u in mass and 30 MeV c.m. in TKE, and over the complete angular range of the PSPP counters (geometries A, B, C, and D in Table I). The center values of the TKE intervals are indicated in the figure. The error bars pertain to statistical uncertainties only. The solid lines are the results of evaporation calculations (see text).

(Ref. 3) and 496-MeV beams.

According to a simple friction model,[23] deep-inelastic collisions involve the conversion of angular momentum of relative motion into intrinsic angular momenta of the fragments. The tangential friction forces may then cause the fragments to be strongly aligned perpendicular to the reaction plane. We computed the upper limit of the neutron out-of-plane anisotropy by assuming the formation of fully aligned states with angular momentum J for which $|M_J| = J$, (Ref. 16). The value of the total angular momentum deposited into the fragments may be estimated from the values of the γ-ray multiplicities measured for ^{86}Kr+^{166}Er at E_{lab} = 515 MeV (Ref. 24) and for ^{86}Kr+^{165}Ho at E_{lab} = 618 MeV (Ref. 25). We obtain average values of ~30$\hbar$, ~44$\hbar$, and ~53$\hbar$ for the total spin of the two fragments in the reaction ^{86}Kr+^{166}Er at E_{lab} = 496 MeV, 602 MeV, and 675 MeV, respectively, for fully damped events. Assuming these angular momenta are shared by the fragments in proportion to their (rigid body) moments of inertia, we expect the heavy fragment to have ~75% of the total spin. Results of the angular distributions as a function of the c.m. out-of-plane angle for ^{86}Kr (E_{ex} = 66 MeV, $J = 13\hbar$) and ^{166}Er (E_{ex} = 128 MeV, $J = 26\hbar$, $36\hbar$, and $50\hbar$) are presented in Fig. 9.

The calculated anisotropy at the position of the out-of-plane counters results from an average over a considerable range of c.m. angles. We estimate the upper limit of this anisotropy to be approximately 20% using the anisotropy curves for ^{86}Kr ($J = 13\hbar$) and ^{166}Er ($J = 36\hbar$). Experimentally, we do not find any evidence for an anisotropy. This could be due in part to the combined syste-

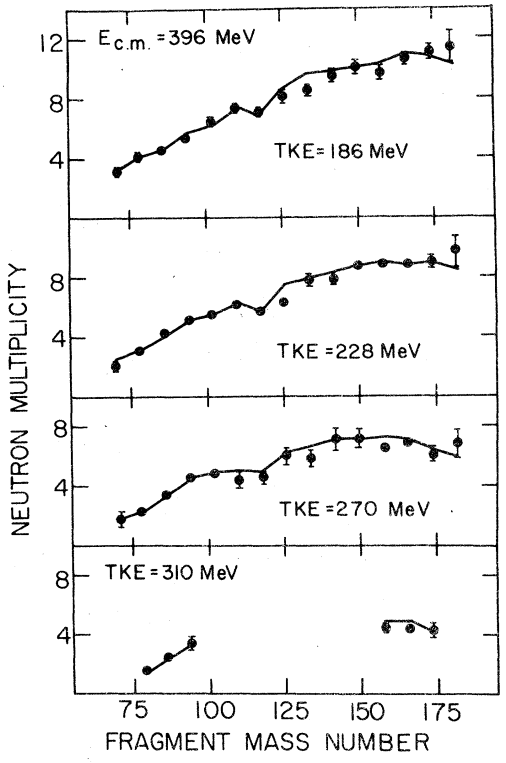

FIG. 7. Neutron multiplicities at four TKE intervals as functions of the fragment primary mass measured for the reaction ^{86}Kr on ^{166}Er at $E_{c.m.} = 396$ MeV. The points were obtained with counters L and R. The neutron multiplicities are averaged over intervals of 8 u in mass and 42 MeV c.m. in TKE, and over the complete angular range of the PSPP counters (geometries *E* and *F* in Table I). The center values of the TKE intervals are indicated in the figure. The error bars pertain to statistical uncertainties only. The solid lines are the results of statistical model calculations (see text).

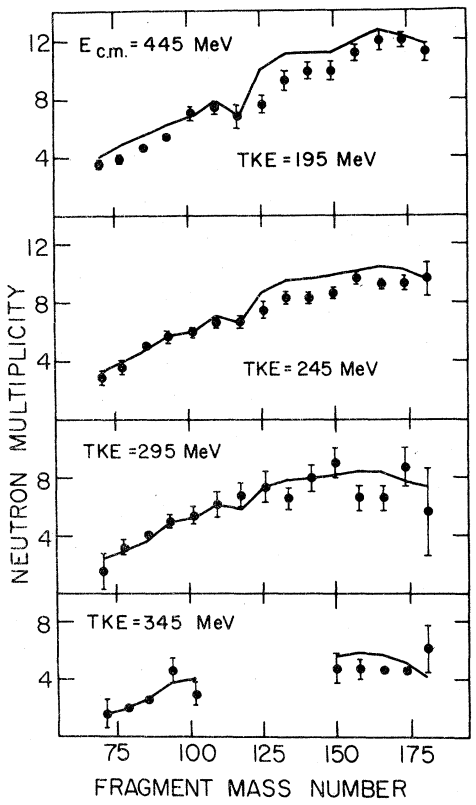

FIG. 8. Neutron multiplicities at four TKE intervals as functions of fragment primary mass measured for the reaction ^{86}Kr with ^{166}Er at $E_{c.m.} = 445$ MeV. The points were obtained with counters L and R. The neutron multiplicities are averaged over intervals of 8 u in mass and 50 MeV in c.m. TKE, and over the complete angular range of the PSPP counters (geometries *G* and *H* in Table I). The center values of the TKE intervals are indicated in the figure. The error bars pertain to statistical uncertainties only. The solid lines are the results of evaporation calculations (see text).

matic errors of ±15% in the detection efficiency of any pair of Ne-213 counters. Therefore, we cannot rule out the possibility that the nuclei are fully aligned. However, recently information on fragment spin alignment in deep-inelastic collisions between very heavy ions has been obtained by employing techniques which involve the detection of sequential fission,[26] γ-ray anisotropies,[27] and γ-ray circular polarization.[28] These experiments suggest that the amount of spin alignment is smaller than the upper limit predicted by the simple friction model.[23] Therefore, we expect the out-of-plane anisotropy to be significantly smaller than quoted above.

B. Neutron multiplicities and neutron energy spectra in the rest frame of the fragments

A quantitative estimate for the amount of excitation energy imparted to the fragments and its partition between the fragments may be obtained by comparing results of evaporation calculations with the data, as shown in Figs. 6–8. The input quantities required by the calculations were chosen in the following manner: (i) for any given mass division the atomic numbers of the light and heavy fragments were taken according to Ref. 12. This choice leads to fragment charge/mass ratios which nearly coincide with the charge/mass ratio of the composite system. (ii) The values of the intrinsic spins of the individual fragments as described in Sec. VIA. (iii) We assumed that the observed TKE loss, corrected for the ground-state *Q* value of the reaction, was transformed into excitation energy of the fragments. (iv) The total excitation energy was divided between the fragments in proportion to their mass.

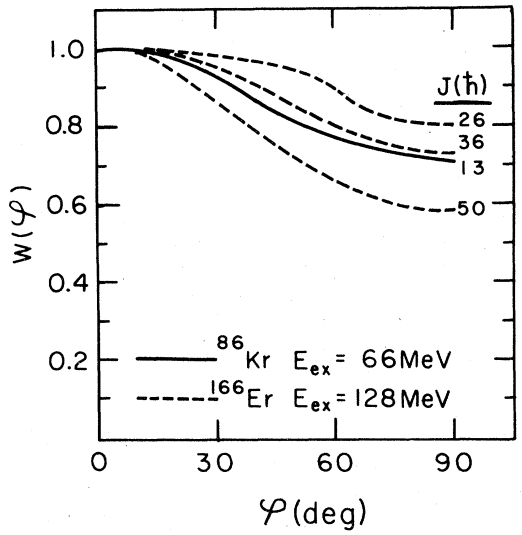

FIG. 9. Angular distributions of neutrons as function of the c.m. out-of-plane angle φ emitted from fragments initially fully aligned perpendicular to the reaction plane. The calculations pertain to ^{86}Kr excited to $E_{ex}=66$ MeV and ^{166}Er excited to 128 MeV with spins J as indicated in the figure.

The calculations show that the de-excitation of all fragments is indeed strongly dominated by neutron emission. The average amount of charge evaporated is <0.4 charge units/fragment. The de-excitation by γ rays is largely suppressed at energies at which particle emission is energetically permitted. The fission probability is essentially negligible even for the heaviest fragments considered in the present work. The dependence of the neutron multiplicity on the fragment spin is weak. We estimate that the calculated values of the neutron multiplicities are accurate within ~0.5 neutrons per fragment for reasonable limits imposed on the predicted fragment charge and angular momentum distributions.

The calculations for the neutron multiplicities are compared with the experimental results in Figs. 6–8. The agreement is generally good for the three bombarding energies over the whole TKE range including the quasi-elastic region. The calculations overestimate slightly the neutron yields of the heavy fragments. This may be due in part to the experimental detection threshold for low energy neutrons which is more important for heavy fragments (see Sec. III B). The small dip in the measured and calculated neutron multiplicities for mass numbers $A \simeq 118$, corresponds to the closed shell $Z=50$. Here the calculations predict a slight increase in the p and α multiplicities at the expense of neutron emission.

Figure 5 compares the measured neutron kinetic energy spectra in the c.m. system of the fragments with the evaporation calculations. The agreement between calculation and data is excellent. In particular, the data show the nearly exponential fall-off with increasing neutron energy, characteristic of statistical decay. The equal temperatures (slopes) of the two fragments indicate energy equilibration in the intermediate system.

VII. CONCLUSIONS

We have reported a study of neutron emission associated with deep-inelastic collisions of ^{86}Kr with ^{166}Er at 5.7-, 7.0-, and 7.9-MeV/nucleon. Neutrons emitted in the reaction plane and out of plane were detected in coincidence with the two complementary heavy reaction fragments. The direct experimental determination of the velocities of the heavy fragments together with their scattering angles allowed the determination of the primary (pre-evaporation) masses and kinetic energies of the fragments, as opposed to a conventional dE/dx-E technique in which the atomic number and final kinetic energy of the fragment is measured. Our measurements involved the determination of neutron yields as a function of bombarding energy, TKE loss, fragment mass, and neutron scattering angles.

Our results show that for the three bombarding energies listed above, the observed TKE loss is transformed into excitation energy of the fragments. The excitation energy is shared between the fragments in proportion to their mass, indicating energy equilibration in the intermediate composite system. The excitation energy is removed mainly by neutron emission from fully accelerated fragments.

We do not observe a component in the forward-angle spectra which may be associated with neutron emission by the intermediate dinuclear complex prior to fragment separation (Fig. 4). Neither do we observe a high-energy component in the neutron c.m. kinetic energy spectra (see Fig. 5), in excess of the evaporation spectra. From the above observations and the agreement between calculated and measured neutron multiplicities and spectra we conclude that within the limits imposed by systematic and statistical uncertainties our data do not show evidence for pre-equilibrium neutron emission. Finally, the observed multiplicity and energy spectra of the neutrons are consistent with predictions of statistical model calculations.

ACKNOWLEDGMENT

We are indebted to Eng. H.J. Beeskow and Dr. H. Spieler for the construction of some of the electronic modules. We thank the staff of the UNILAC accelerator for delivering a bunched Kr beam of excellent quality. One of us (C.R.G.) acknowledges the receipt of an Alexander von Humboldt Fellowship. This work was supported in part by Bundesministerium für Forschung und Technologie, Federal Republic of Germany.

---

*On leave from North Carolina State University.
†Present address: Max Planck Institut für Kernphysik, Heidelberg, West Germany.

[1]J. Peter, M. Berlanger, C. Ngo, B. Tamain, B. Lucas, C. Mazur, M. Ribrag, and C. Signarbieux, Z. Phys. A283, 413 (1977).
[2]C. R. Gould, R. Bass, J. Czarnecki, V. Hartmann, K. Stelzer, R. Zitzmann, and Y. Eyal, Z. Phys. A284, 353 (1977).
[3]Y. Eyal, A. Gavron, I. Tserruya, Z. Fraenkel, Y. Eisen, S. Wald, R. Bass, C. R. Gould, G. Kreyling, R. Renfordt, K. Stelzer, R. Zitzmann, A. Gobbi, U. Lynen, H. Stelzer, I. Rode, and R. Bock, Phys. Rev. Lett. 41, 625 (1978).
[4]D. Hilscher, J. R. Birkelund, A. D. Hoover, W. U. Schroder, W. W. Wilcke, J. R. Huizenga, A. Mignerey, K. L. Wolf, H. F. Breuer, and V. E. Viola, Jr., Phys. Rev. C 20, 576 (1979).
[5]B. Tamain, R. Chechick, H. Fuchs, F. Hanappe, M. Morjean, C. Ngo, J. Peter, M. Dakowski, B. Lucas, C. Mazur, M. Ribrag, and C. Signarbieux, Nucl. Phys. A330, 253 (1979).
[6]F. Plasil, R. L. Ferguson, H. C. Britt, R. H. Stokes, B. H. Erkkila, P. D. Goldstone, M. Blann, and H. H. Gutbrod, Phys. Rev. Lett. 40, 1164 (1978).
[7]R. Babinet, B. Cauvin, J. Giraud, H. Nifenecker, B. Gatty, D. Guerreau, M. Lefort, and X. Tarrago, Nucl. Phys. A296, 160 (1978).
[8]B. Gauvin, R. C. Jared, P. Russo, R. P. Schmitt, R. Babinet, and L. G. Moretto, Nucl. Phys. A301, 511 (1978).
[9]R. P. Schmitt, G. Bizard, G. J. Wozniak, and L. G. Moretto, Phys. Rev. Lett. 41, 1152 (1978).
[10]Y. Eyal and H. Stelzer, Nucl. Instrum. Methods 155, 157 (1978).
[11]Data acquisition system JUHU, developed by U. Lynen.
[12]Y. Eyal, G. Rudolf, I. Rode, and H. Stelzer, Phys. Rev. Lett. 42, 826 (1979).
[13]A. Gavron, Nucl. Instrum. Methods 115, 99 (1974).
[14]M. Drosg, Nucl. Instrum. Methods 105, 582 (1972).
[15]Z. Fraenkel, I. Mayk, J. P. Unik, A. J. Gorski, and W. D. Loveland, Phys. Rev. C 12, 1809 (1975).
[16]Monte Carlo statistical-model code JULIAN, M. Hillman and Y. Eyal (unpublished), modified by A. Gavron to couple angular momentum projections.
[17]L. Rosen, J. G. Beerg, A. S. Goldhaber, and E. H. Auerbach, Ann. Phys. (N.Y.) 34, 96 (1965); C. M. Perey and F. G. Perey, Nucl. Data Tables 17, 1 (1976).
[18]J. R. Huizenga and G. Igo, Nucl. Phys. 29, 462 (1962).
[19]F. Bertrand, M. Martinot, and N. Verges, in *Nuclear Data in Science and Technology* (IAEA, Vienna, 1973), Vol. II, p. 353.
[20]A. M. Zebelman, L. Kowalski, J. Miller, K. Beg, Y. Eyal, G. Yaffe, A. Kandil, and D. Logan, Phys. Rev. C 10, 200 (1974).
[21]S. Cohen, F. Plasil, and W. J. Swiatecki, Ann. Phys. (N.Y.) 22, 406 (1973).
[22]A. Gilbert and A. G. W. Cameron, Can. J. Phys. 43, 1446 (1965).
[23]J. Wilczynski, Phys. Lett. 47B, 484 (1973).
[24]A. Olmi, H. Sann, D. Pelte, Y. Eyal, A. Gobbi, W. Kohl, U. Lynen, G. Rudolf, H. Stelzer, and R. Bock, Phys. Rev. Lett. 41, 688 (1978).
[25]M. M. Aleonard, G. J. Wozniak, P. Glassel, M. A. Deleplanque, R. M. Diamond, L. G. Moretto, R. P. Schmitt, and F. S. Stephens, Phys. Rev. Lett. 40, 622 (1978).
[26]P. Dyer, R. J. Puigh, R. Vandenbosch, T. D. Thomas, and M. S. Zisman, Phys. Rev. Lett. 39, 392 (1977); G. J. Wozniak, R. P. Schmitt, P. Glassel, R. C. Jared, G. Bizard, and L. G. Moretto, *ibid.* 40, 1436 (1978).
[27]R. Bock, B. Fisher, A. Gobbi, K. Hildenbrand, W. Kohl, U. Lynen, I. Rode, H. Stelzer, G. Auger, J. Galin, J. M. Lagrange, B. B. Back, and R. Albrecht, Nukleonika 22, 529 (1977); C. Gerschel, M. A. Deleplanque, M. Ishihara, C. Ngo, N. Perrin, J. Peter, B. Tamain, L. Valentin, D. Paya, Y. Sugiyama, M. Berlanger, and F. Hanappe, Nucl. Phys. A317, 473 (1979); R. Dayras, R. G. Stokstad, C. B. Fulmer, D. C. Hensley, M. L. Halbert, D. G. Sarantites, L. Westerberg, and J. H. Barker, Phys. Rev. Lett. 42, 697 (1979).
[28]W. Trautmann, J. de Boer, W. Dunnweber, G. Graw, R. Kopp, G. Lauterbach, H. Puchta, and U. Lynen, Phys. Rev. Lett. 39, 1062 (1977).